

Effect of temperature on the optical properties of $\text{Ag}_3\text{O}_4/\text{AgO}$ thin films

Uche Eunice EKPUNOBI, Chikaodili Anthonia AKUMUO, Adaora Stellamarris
OGBUAGU, Chiamara Blessing DURU and Vincent Ishmel Egbulefu AJIWE

*Pure and Industrial Chemistry Department, Nnamdi Azikiwe University, P.M.B. 5025, Awka,
Anambra State. Nigeria*
E-mail(*): ask4uche2001@yahoo.com

* Corresponding author, phone: +2348037614963

Abstract

Silver oxide (Ag_2O_3) thin films of optical thicknesses $0.1\mu\text{m}$ to $0.4\mu\text{m}$ were electrodeposited on a transparent fluorine-doped tin oxide (FTO) conducting glass substrate at room temperature from the silver solution. When the temperature of the solution was increased to 50°C , the films optical thicknesses also increased ranging from $0.26\mu\text{m}$ to $0.44\mu\text{m}$. The films gave a monoclinic structures of Ag_3O_4 and AgO films of (031) and (111) planes of reflections. Other optical measurements like absorbance, optical conductivity and extinction coefficient at 50°C show increase in percentage when compared with the properties of the silver oxide thin films deposited at room temperature. The band gap decreased as the films thicknesses increased.

Keywords

Silver oxide thin films; Optical conductivity; Extinction Coefficient

Introduction

A number of researchers have deployed silver (Ag) nanoparticles through a number of techniques on various substrates including carbon, zeolites and polymers for water

disinfection applications [1,2]. However, Ag impregnated on an inorganic fiberglass surface through a simple electrolytic process was only recently reported for the first time [3]. Fiberglass impregnated with Ag nanoparticles displays superior performance over carbon-based silver support systems in terms of architecture of the system, its interfacial properties and its bactericidal activity [1]. Ag_xO thin films have been widely studied due to their wide range of applications such as heat-reflecting mirrors, chemical sensors, split-dipole nano-antennas [3]. Highly (101)-oriented p-Ag₂O thin film with high electrical resistivity was grown by rapid thermal oxidation (RTO) on clean monocrystalline p-type Si without any post-deposition annealing. From optical transmittance and absorbance data, the direct optical band gap was found to be 1.46 eV. The electrical and photovoltaic properties of Ag₂O/Si isotype heterojunction were examined in the absence of any buffer layer. Ideality factor of heterojunction was found to be 3.9. Photoresponce result revealed that there are two peaks located at 750 nm and 900 nm. The spectral distribution of photoconductivity in Ag₂O was measured on samples prepared in three different ways. The photoresponse was found to depend on the mode of preparation of samples and on previous light exposure [4-6]. Samples prepared by pressing Ag₂O powder against a cellulose backing showed a photoconductive peak around 0.9μm, while thin Ag₂O layers prepared by cathodic sputtering of silver in an oxygen atmosphere behaved like the ideal photoconductors: flat response in the visible and exponential decrease from 0.8μm to longer wavelengths [7]. The semiconducting and photovoltaic properties of p-type Ag₂O films grown anodically on silver electrodes were studied, in view of possible applications in solar energy conversion. Films were grown in different alkaline solutions; the best results were obtained for 0.02M Ag₂SO₄ + 0.17M NH₄OH + 5.7 × 10⁻³M Ba(OH)₂ saturated with Ag₂O powder, stirred mechanically at room temperature [8,9]. Film thicknesses of up to 10μm were thus obtained for the first time in anodically grown Ag₂O. Photovoltaic spectra taken at 300 K give a bandgap of $E_g = 1.42 \pm 0.04$ eV. Evaporated gold on Ag₂O apv pears to be ohmic while aluminium and platinum are rectifying. The barrier height of Ag/Ag₂O is 0.90 ± 0.02 eV, that of Al/Ag₂O is 0.93 ± 0.02 eV, and that of platinum 0.94 ± 0.02 eV. The best cells give an open-circuit voltage, V_{oc} , of over 150 mV, and a short circuit current, $I_{sc} = 100\mu A \text{ cm}^{-2}$ under 50mW cm^{-2} illumination. Silver has long been used for mirrors and tableware due to its high reflectivity, and it is still a very important component in optics. In particular, silver xsisland films or small particles have been applied as photographic materials, tools and devices to generate localized electrical

fields for molecular detection and electrical field enhancement. It has recently been discovered that silver oxide thin films may be a very useful material for dealing with optical near-field and surface plasmons [10]. Silver oxide decomposes into oxygen and small metallic silver particles, and this characteristic has been applied to ultrahigh-density optical data storage to create a strong light-scattering center that resolves small pits or marks beyond the diffraction limit [11]. More recently, it has been found that silver film can be cheaply and easily transformed into Ag nanoparticles and nanowires in a gas mixture of hydrogen and oxygen in a vacuum chamber [12,13]. The particle and wire diameters are very uniform and approximately 20-50nm, and they can be three-dimensionally fabricated on almost all material surfaces without the need for thermal annealing. Silver nanoparticles and wires will soon appear in small and cheap molecular detection sensors by small precise adjustments for generating surface plasmon conditions [14]. In this work, oxides of silver were deposited on conducting glass substrates by electrodeposition from solutions of silver recovered from waste. The optical, structural and morphological properties of the deposited films were studied. The effect of temperature on the optical properties of the films was also calculated.

Material and method

Experiments

Used x-ray films were collected from Anambra State University Teaching Hospital, Awka, Anambra State, Nigeria. The waste x-ray films were cut into small pieces (2×2cm). 200g was weighed into a beaker. The weighed waste x-ray films were added to 10ml of 1M nitric acid (HNO₃) in a 1000ml beaker and shaken to allow uniform dissolution of the silver compounds. The mixture was stirred for 30mins at 26°C. Another setup as described above was made and the mixture was stirred continuously at a temperature of 50°C on a hot plate. At the end of the set time, the polyethylene plates were washed with 20ml of distilled water each to ensure no loss of any silver solution [14]. The resultant solutions were labeled A, and B respectively.

Deposition

Preparation of the silver oxide films on the FTO transparent conducting glass substrate was carried out using the electrodeposition technique. 10ml each of the resultant solutions A,

and B was used for electrodeposition with temperature of solution B maintained at 50°C. FTO (Fluorine doped Tin Oxide) coated transparent glass of dimension 25mm×25mm×3mm was used as the cathode while a carbon electrode was used as the anode. The electrodeposition was done under 4V and 20 secs at room temperature (26°C). The pH values of the solutions were recorded. Deposition was repeated at various voltages (1V, 2V, and 3V) with time kept constant but no visible or appreciable result was obtained. At the end of electrodeposition, the coated substrates were washed well with distilled water and air dried at room temperature.

Characterization

The electrolyte solutions A, and B before and after electrodeposition were analyzed using Atomic Absorption Spectrometer (AAS). The dried substrates were taken for topographical and structural characterization using photomicrograph (*60 magnification) and XRD (x-ray minidiffractometer 10). The optical properties of the samples were examined using UltraViolet-Visible spectrophotometer at the normal incident of light in the wavelength range 350-700nm. From the absorbance recorded from the UV readings, other optical parameters like transmittance, reflectance, refractive index, extinction coefficient, absorption coefficient squared, optical conductivity, real dielectric constant and imaginary dielectric constant were calculated.

The equation relating refractive index to reflectance and extinction coefficient [15, 16] was used in the calculations as shown in equation (1).

$$R = \frac{(n-1)^2 + k^2}{(n+1)^2 + k^2} \quad (1)$$

where R is the reflectance, n, refractive index and k, the extinction coefficient. When k is $\ll n^2$, the relationship, the equation approximates to:

$$n = \frac{1 + R^{\frac{1}{2}}}{1 - R^{\frac{1}{2}}} \quad (2)$$

The absorption coefficient was calculated using equation (3)

$$\alpha = \frac{\ln\left(\frac{1}{T}\right)}{d} \quad (3)$$

The result of the optical thickness calculated using equation (4) according to report [15] showed that the films are thin films.

$$t = (\ln[(1-R)n/T])/\alpha \quad (4)$$

According to a report [15], energy band gaps, E_g , are calculated using equation (5):

$$E_g = hf - \alpha^2 \quad (5)$$

where E_g is the energy band gap, h is planck's constant, f is the frequency of radiation and α^2 is the coefficient of absorption squared. The band gaps were determined by plotting a graph of absorption coefficient squared versus photon energy and sequent extrapolation of the straight line to meet the photon energy

Results and discussion

AAS analysis

In Table 1 is shown the AAS analysis of the electrolyte solutions for silver before and after electrodeposition. From the table it was observed that recovery of silver from waste was higher when the temperature was increased and also enhanced better deposition with respect to the changes in concentration after electrodeposition.

Table 1. AAS analysis of the electrolyte solutions before and after electrodeposition

Sample	Before Electrodeposition		After Electrodeposition	
	Absorbance	Concentration(ppm)	Absorbance	Concentration(ppm)
A (X-ray + HNO ₃ + 26°C)	0.007	6.50	0.005	6.00
B (X-ray + HNO ₃ + 50°C)	0.012	10.00	-	-

Structural characterization by X-ray diffraction

Figure 1a shows the x-ray diffraction spectra of silver oxide thin films deposited from electrolyte A (X-ray + HNO₃) at room temperature (26°C). The figure reveals the existence of six (6) prominent peaks of orientation (110), (031), (111), (121), (023), (240) planes of reflections. The reflections gave intergrowths of monoclinic structures of Ag₃O₄ (031) and AgO (111) planes of reflections. The crystals were sharp at inter planar distance of 3.24983Å and collapsed at 1.37156 Å. The average crystalline grain size calculated is 5.426Å and 0.26µm thickness.

Ag_3O_4 could be recognized as a compound consisted of Ag_2O_3 and AgO^* , where * is the sign for this AgO in order to distinguish the AgO produced during the reaction process. In low rate discharge process Ag_2O_3 could transform to AgO and then further reduced to Ag_2O , until became it metal Ag [17-21].

In Figure 1b shows the x-ray diffraction spectra of silver oxide thin films deposited from electrolyte B (X-ray + HNO_3) at room temperature ($50^\circ C$). The figure reveals the existence of three (3) prominent peaks of orientation (110), (031), and (111) planes of reflections. The reflections gave intergrowths of monoclinic structures of Ag_3O_4 (031) and AgO (111) planes of reflections. The crystals were sharp at inter planar distance of 3.24751 \AA and collapsed at 1.69355 \AA . The average crystalline grain size calculated is 5.273 \AA and $0.44\text{ }\mu m$ thickness.

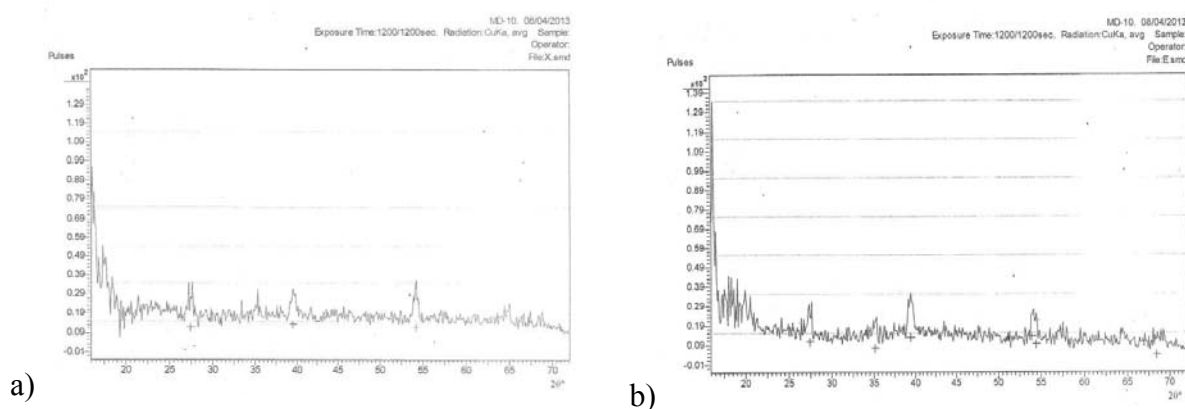


Figure 1. The XRD pattern of the deposited Ag_xO films from Electro: a) at $26^\circ C$ and b) at $50^\circ C$

Topographical characterization

The topographical characterization of the films deposited was studied in order to determine the small changes in the surface contour of films (lattice surface defects) like dislocations, stacking faults, etc. as well evaluating the whole image field. Figures 2a and 2b show the micrograph of the films deposited from electrolytic solutions A, and B respectively. From the Figures, it is deduced that the crystals have a good cluster with that from electrolyte A giving the best nucleation.

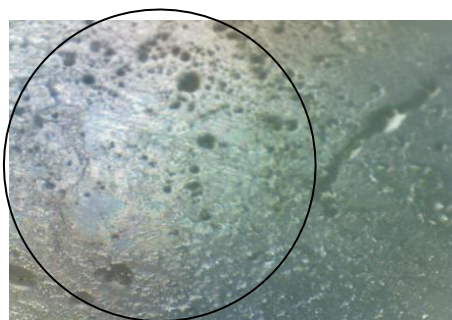


Figure 2a. Micrograph of films from sample A (26°C)

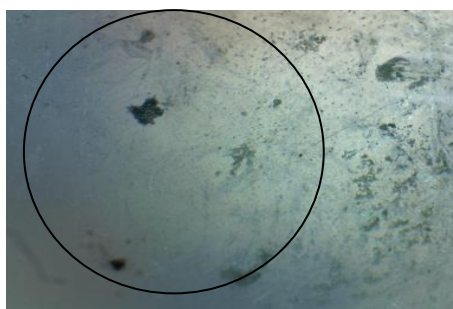


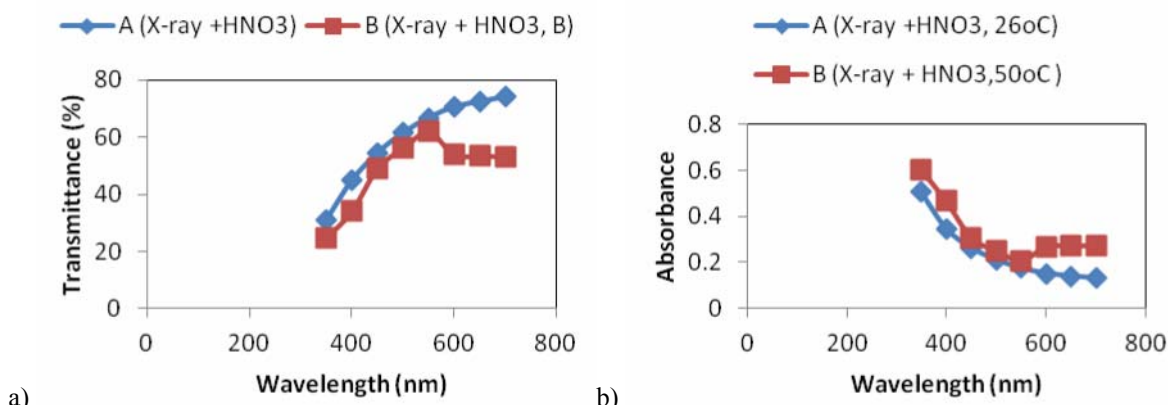
Figure 2b. Micrograph of films from sample B (50°C)

Optical studies

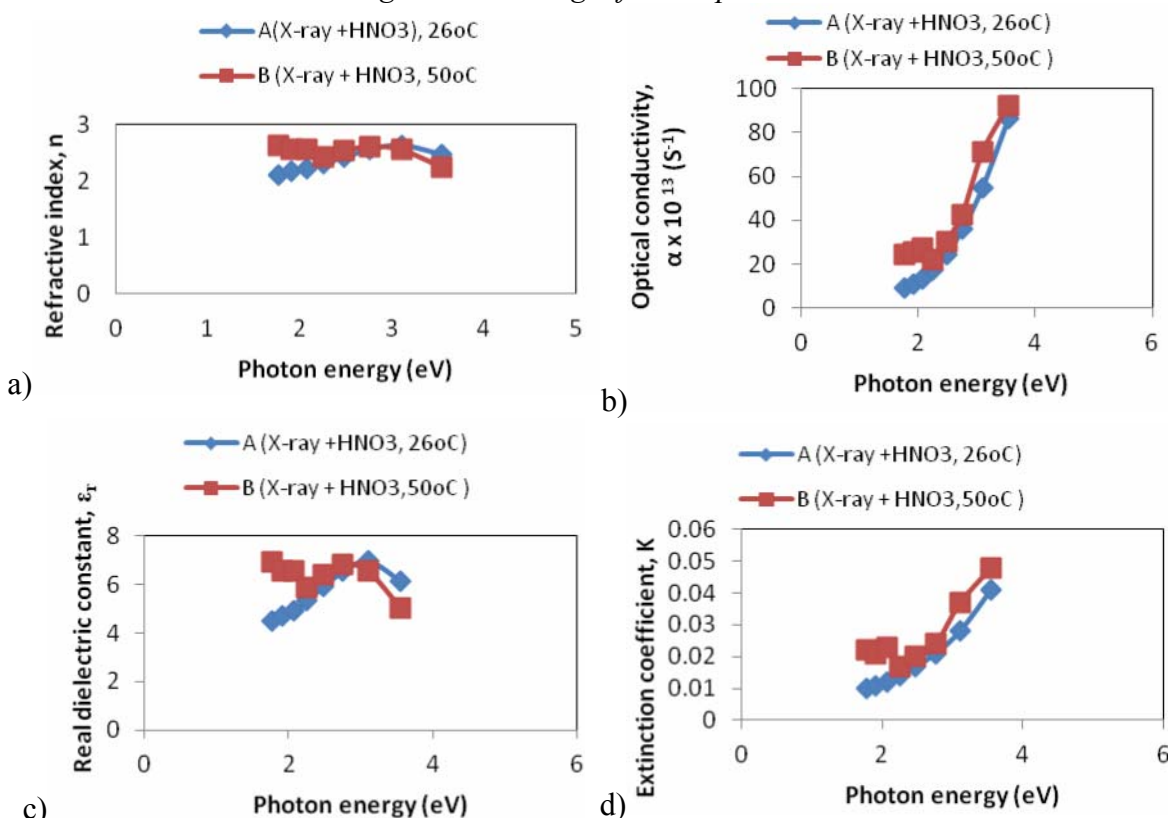
Figure 3a shows the absorbance plot as a function of wavelength as obtained from the UV-VIS spectrophotometer for all the electrolytic solutions studied. The transmittance and reflectance were calculated using Beer Lamberts equations [22-24], assuming negligible scattering as shown in Figure 3b and 3c. The films all showed high absorbance in the visible region with absorption edges in the blue region of the electromagnetic spectrum. In a report of synthesis of silver oxide and its photoactivation, it was discovered that photoactivation of silver oxides in this region causes transition from ground to excited state. The electrons transit to the energy level of the impurities induced by photocatalytic centers (Ag_3O , $\text{AgO}_2 + \text{O}$, and $\text{Ag}_3 + \text{O}$) when being photoactivated by blue light. This is why illumination of silver samples with blue and UV mercury lamp produces fluorescent Ag_x nanoclusters [22]. This phenomenon of Ag_xO is what makes it suitable for Surface Enhanced Raman Scattering detection (SERS) for chemical and biological molecules and optical data storage [23]. From the results, it was seen that electrolytic solution A(X-ray + HNO_3 + 50°C) gave a better absorption than B (X-ray + HNO_3 + 26°C) whereas with transmittance, the order is reversed. The average percentage of transmittance of films from sample B was 63% whereas that of sample A was 51.8%. This implies that at lower temperature the films produced were more

transparent than at higher temperature. A look at the Figure 3c showed that sample B had a higher reflectance than sample A.

Plots of refractive index, extinction coefficient and optical conductivity are shown in Figures 4a, 4b and 4c respectively. The maximum optical conductivity could be detected from Fig. 4b to be $3.545eV$.



a) *Figure 3. a) A plot of Absorbance Vs wavelength for samples A; b) A plot of transmittance against wavelength for samples A-B*



a) *Figure 4. a. A plot of refractive index against photon energy for samples A – B; b. A plot of optical conductivity against photon energy for samples A – B; c. A plot of extinction coefficient against photon energy for samples A – B; d. A plot of real dielectric constant against photon energy for samples A – B;*

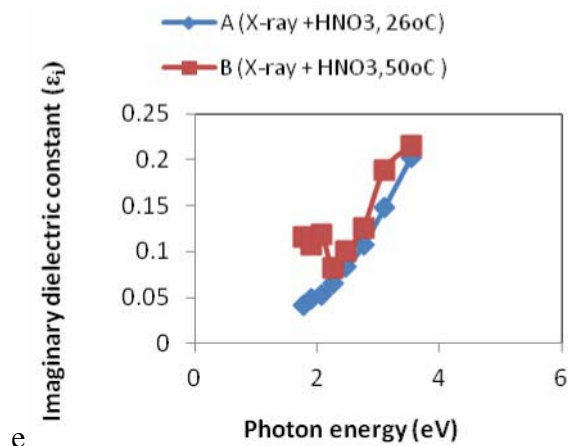


Figure 4. e. A plot of imaginary dielectric constant against photon samples A – B

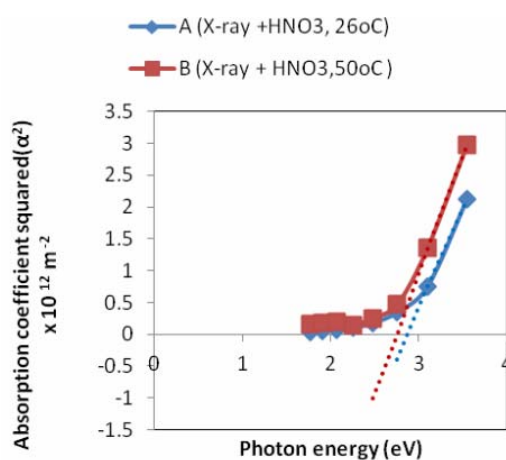


Figure 5. Plot of direct energy band gap for samples A – B

Plotting the absorption coefficient squared as a function of photon energy, energy band gap was measured from the intercept (tangent value). The band gaps obtained from the plots are 2.900eV, and 2.757eV for samples A, and B respectively. These compared well with other values from report as follows; Raju et al, 1.01 – 0.93eV, Fortiu and Weichman, 1.2eV [24], Ramesh et al., 3.5eV, Nwanya et al., 1.64 – 1.95eV, etc [15]. There is indeed a wide difference which could be from the varied methods employed.

Conclusions

Silver oxide films were successfully deposited on FTO transparent conducting glass solutions of silver recovered from waste at different temperatures. The films deposited from electrolyte B (X-ray + cassava + 26°C) are more transparent when compared to films from electrolyte A (X-ray + cassava + 50°C) but other optical properties studied showed that films

from higher temperature environment had higher values than those of the lower temperature. Both films gave an intergrowth of Ag₃O₄ and AgO which was relatively more transparent than others. The results of the optical properties calculated show that the silver oxide deposited could find usage in silver oxide and rechargeable batteries, photovoltaic applications and as semiconductors.

Acknowledgements

The authors appreciate the support of Anambra State Teaching hospital, Awka in providing the used x-ray films and Centre for Energy Research & Development, Obafemi-Awolowo University, Ile-Ife, Nigeria for assistance in characterization

References

1. Nangmenyi G., Yue Z., Mehrebi S., Mintz E., Economy J., *Synthesis and characterization of silver-nanoparticle-impregnated fiberglass and utility in water disinfection*. Nanotechnology, 2009, 20(49), 495705.
2. Nieto A., Borrull F., Pocurull E., Marcé R. M., *Pressurized liquid extraction: a useful technique to extract pharmaceuticals and personal-care products from sewage sludge*, Trends in Analytical Chemistry, 2010, 29(7), p. 752-764.
3. Syed S., Sharma L. M., Syed A. A. *Clean technology for the recovery of silver from processed radiographic films*. Hydrometallurgy, 2002, 63(3), p. 277-280.
4. Garcia R. M. *The recovery of silver from photographic film: A study of the leaching reaction with cyanide solution for industrial use*, Hydrometallurgy, 1986, 16, p. 395-400.
5. Qu Z, Cheng M., Dong X., Bao X., *CO selective oxidation in H₂-rich gas over Ag nanoparticles-effect of oxygen treatment temperature on the activity of silver particles mechanically mixed with SiO₂*, Catal. Today., 2004, 93, p. 247-255.
6. Chakravorty D., Basu S., Mukherjee P. K., Saha S. K., Pal B. N., Dan A., Bhattacharya S. *Novel properties of glass-metal nanocomposites*, J. Non-Cryst. Solids., 2006, 352(6-7), p. 601-609.
7. Varanda L. C., Morales M. P., Goya G. F., Imaizumi M., Serna C. J., Jafelicci M.

- Magnetic properties of acicular Fe_{1-x}RE_x (RE = Nd, Sm, Eu, Tb; x = 0, 0.05, 0.10) metallic nanoparticles*, Mater. Sci. Eng. B., 2004, 112(2-3), p. 188-193.
8. Basu S., Chakravorty D. *Optical properties of nanocomposites with iron core-iron oxide shell structure*, J. Non-Cryst. Solids, 2006, 352(5), p. 380-385.
 9. Fujiwara N., Tsumiya T., Katada T., Hosobuchi T., Yamamoto K. *Continuous recovery of silver from used X-ray films using a proteolytic enzyme*, Process Biochemistry, 1989, 24, p. 155-156.
 10. Ishikawa H., Ishimi K., Sugiura M., Sowa A., Fujiwara N., *Kinetics and mechanism of enzymatic hydrolysis of gelatin layers of X-ray film and release of silver particles*. Journal of Fermentation and Bioengineering, 1993, 76(4), p. 300-305.
 11. Laxman R. S., Sonawane A. P., More S. V., Rao B. S., Rele M. V., Jogdand V. V., Deshpande V. V., Rao M. B. *Optimization and scale up of production of alkaline protease from Conidiobolus coronatus*, Process Biochemistry, 2005, 40, p. 3152-3158.
 12. Lowry O. H., Rosebrough N. J., Farr A. L., Randall R. J., *Protein measurement with the folin phenol reagent*, Journal of Biological Chemistry, 1951, 193, p. 265-275.
 13. Masui A., Fujiwara N., Takagi M., Imanaka T., *Feasibility study for decomposition of gelatin layers on X-ray films by thermostable alkaline protease from alkaliphilic Bacillus sp.*, Biotechnological Techniques, 1999, 13, p. 813-815.
 14. Masui A., Yasuda M., Fujiwara N., Ishikawa H. *Enzymatic hydrolysis of gelatin layer on used lith film using thermostable alkaline protease for the recovery of silver and PET film*, Biotechnology Progress, 2004, 20, p. 1267-1269.
 15. Chopra K. L., Malhotra L. K., Eds., *Optical Properties of Thin Films*, Tata McGraw-Hill, 1985, New Delhi, India.
 16. Nwanya A. C., Ugwuoke I. P. E., Ezekoye I. B. A., Osuji R. U., Ezema F. I., *Structural and Optical Properties of Chemical Bath Deposited Silver Oxide Thin Films: Role of Deposition Time*, Advances in Materials Science and Engineering, 2013, 2013, Article ID 450820.
 17. Nakiboglu N., Toscali D., Nisli G. *A novel silver recovery method from waste photographic films with NaOH stripping*, Turk Journal of Chemistry, 2003, 27, p. 127-133.
 18. Nakiboglu N., Toscali D., Yasa I., *Silver recovery from waste photographic films by an enzymatic method*, Turk Journal of Chemistry, 2001, 25, p. 349-353.

19. Marinković J. I., Korać M., Kamberović Ž., Matić I., *Recycling of silver from exposed x-ray films*, Acta Metallurgica Slovaca, 2006, 12, 262-268.
20. Shankar S., More S. V., Seeta L. R., *Recovery of silver from waste x-ray film by alkaline protease from Conidiobolus coronatus*, Kathmandu University Journal of Science, Engineering and Technology, 2010, 6(I), p. 60-69.
21. Ullash K. S., Srinivasan S., Nagendra C. L., Subrahmanyam A. *Electrical and optical properties of reactive DC magnetron sputtered silver oxide thin films: role of oxygen*, Thin Solid Films, 2003, 429(1-2), p. 129-134.
22. Xiao-Yong G., Song-You W., Jing L., Yu-Xiang Z., Rong-Jun Z., Peng Z., Yue-Mei Y., Liang-Yao C. *Study of structure and optical properties of silver oxide films by ellipsometry, XRD and XPS methods*, Thin Solid Films, 2004, 455-456, p. 438-442.
23. Nabil B., Abdelaziz R., Ouennoughi Z., Douara A. *Fabrication and characteristics of Hg/n-bulk GaN schottky diode*, Leonardo Journal of Sciences, 2015, 26, p. 113-123.
24. Ekpunobi U. E., Anozie A. I., Okwukogu O. O., Ogbuagu A. S., Ajiwe V. I. *Deposition and Characterization of Silver Oxide from Solution of Silver, Cassava and Sugarcane Juice Effects*, Leonardo Journal of Sciences, 2013, 22, p. 21-28.